

Hepatic Arterial Embolization Using Cone Beam CT with Tumor Feeding Vessel Detection Software: Impact on Hepatocellular Carcinoma Response

F. H. Cornelis^{1,2} · A. Borgheresi¹ · E. N. Petre¹ · E. Santos¹ · S. B. Solomon¹ · K. Brown¹

Received: 26 May 2017 / Accepted: 24 July 2017 / Published online: 2 August 2017

© Springer Science+Business Media, LLC and the Cardiovascular and Interventional Radiological Society of Europe (CIRSE) 2017

Abstract

Purpose Dedicated tumor feeding vessel detection software (TFVDS) using cone beam CT has shown a higher sensitivity to detect tumor feeding vessels during hepatic arterial embolization (HAE) of hepatocellular carcinoma (HCC) compared to 2D imaging. Our primary hypothesis was that HCC tumors treated with HAE guided by a TFVDS would show more complete response (CR) than when treated with 2D imaging alone. Secondary analysis of the impact on X-ray exposure was performed.

Materials and Methods Nineteen males and 8 females (median age: 69 year, 46–85) with 44 tumors (median size: 38 mm, 6–100) treated with selective HAE between January 2013 and December 2014 were included. Exclusion criteria were: extra-hepatic supply, >4 tumors, tumor size >10 cm, and adjunctive local therapy. Baseline patient and procedure characteristics were reviewed. Differences in CR per modified Response Evaluation Criteria in Solid Tumors were assessed by univariate and multivariate analyses for tumor size, number, location, particles size, and use of TFVDS.

Results Median imaging follow-up was 20.1 months (2–33). Use of TFVDS (13 patients, 19 tumors) was the only factor predictive of CR (OR = 3.85 [CI95%: 1.09, 13.67], $p = 0.04$) on univariate analysis but not on multivariate analysis (OR = 3.26 [0.87, 12.23], $p = 0.08$). A

higher rate of CR was observed for HAE using TFVDS guidance versus 2D imaging alone (68.4%, 13–19, vs. 36%, 9–25, $p = 0.03$). Median dose area product was lower when TFVDS was used (149.7 Gy.cm², 38–365, vs. 227.8 Gy.cm², 85.3–468.6, $p = 0.05$).

Conclusions HCC embolized with TFVDS may result in improved local tumor response without increasing the dose exposure.

Keywords Hepatic arterial embolization · Cone beam computed tomography · Automated vessel tracking · Tumor response

Introduction

For patients who undergo hepatic arterial embolization (HAE) of hepatocellular carcinoma (HCC), the literature suggests that the efficiency and success of the treatment are mainly dependent upon the ability of the interventional radiologist to perform selective or super-selective embolization [1]. It is purported that the ischemic effect due to embolization itself has a more central role in the treatment than the local effect due to a drug [2, 3]. As such, while embolization procedures can include delivery of a drug to the cancer, more precise selective techniques may improve the clinical outcomes of patients.

In the angiography suite, imaging technology is used to assist the interventional radiologist in selecting vessels of interest for embolization. Cone beam computed tomography (CBCT) has been integrated for several years into the angiography suite allowing real-time 3D image acquisition during procedures [4]. Its use has been associated with improved patient survival compared with 2D digital subtraction angiography (DSA) [5].

✉ K. Brown
brown6@MSKCC.ORG

¹ Department of Radiology, Interventional Radiology Service, Memorial Sloan Kettering Cancer Center, 1275 York Avenue, New York, NY 10065, USA

² Department of Radiology, Tenon Hospital, APHP, 4 rue de la Chine, 75020 Paris, France

More recently, the integration of tumor feeding vessel detection software (TFVDS) has been of interest. TFVDS can extract potential segmental or sub-segmental tumor feeding vessels from a CBCT dataset. It detects vessels with even higher sensitivity and positive predictive value compared with either DSA or CBCT alone [6–9]. Used by X-ray technologists alone, it can exhibit higher sensitivity for vessel detection compared with the manual review of CBCT images by interventional radiologists [10]. In addition, TFVDS may also help reduce the total number of image acquisitions as well as decrease the procedural time while maintaining a comparable treatment efficacy as compared to procedures done without TFVDS [11].

While the use of TFVDS has shown much promise in identifying vessels of interest, there is a lack of literature evaluating its relationship with clinical outcomes. Thus, the overall purpose for this study was to determine the clinical outcomes of using TFVDS versus DSA alone in HAE treatment of HCC tumors. We hypothesized that HCC tumors treated with HAE guided by TFVDS would show a higher rate of complete treatment, leading to a higher rate of complete response. The impact of the use of TFVDS on X-ray dose exposure and procedure time was also evaluated as part of the study.

Materials and Methods

This retrospective study was conducted at a tertiary cancer institution and was approved by our Institutional Review Board who provided a waiver of informed consent. We performed this study in accordance with the Health Insurance Portability and Accountability Act.

Patient Study Selection

We designed patient selection for this study to (1) isolate a group of patients presenting with HCC who may benefit from assistance in identifying vessels supplying the tumor that arise from the common hepatic artery and (2) exclude those in whom non-selective lobar embolization would be used or where extra-hepatic vessels were likely to supply the tumor based on pre-procedure imaging or tumor location.

In this sequential retrospective single-institution study, we searched our institutional database for all HCC patients undergoing a HAE procedure between January 2013 and December 2014. This period overlapped with an Institutional Review Board-approved phase II clinical trial evaluating the feasibility of TFVDS in clinical practice. This phase II clinical trial used the following inclusion criteria: unresectable hypervascular HCC or liver metastases with at least one hypervascular lesion planned for selective HAE.

Patients undergoing HAE were treated using TFVDS guidance or DSA only during this period.

The diagnosis of HCC was confirmed by either liver biopsy or applying European Association for Study of the Liver criteria to dynamic contrast-enhanced CT or MR imaging [12]. A multidisciplinary liver tumor conference discussed the treatment plan for each patient before each patient was treated. Eligibility criteria for HAE were as follows: unresectable HCC, Child–Pugh classification A or B, Eastern Cooperative Oncology Group performance status 0 or 1, and no contraindication to contrast medium.

We applied the following patients' inclusion criteria to minimize the number of variables impacting the clinical outcomes for this study: patients receiving their first HAE treatment, maximal diameter of lesion ≤ 10 cm, and patients with follow-up CT imaging at least 4 weeks post-HAE. Patients' exclusion criteria were: patients presenting with extra-hepatic vessels supplying the tumor, more than 4 tumors and patients undergoing additional local therapy (ablation or percutaneous alcohol injection) the day of the treatment. In addition, patients must undergo either selective or super-selective embolization. Documentation of a selective procedure was done by review of the images as well as reports for the procedure.

Hepatic Arterial Embolization

Embolization procedures were performed according to the standard protocol previously described by Brown et al. [13]. Bland embolization was proposed based on existing evidence from randomized controlled trials that bland transarterial embolization has the same efficacy compared to transarterial chemoembolization [14, 15]. All embolization procedures using either DSA or TFVDS were performed by 5 interventional radiologists with 10–20 years of experience in hepatic interventions. Briefly, using the Seldinger's technique, visceral angiography was performed via the common femoral artery with a 4- or 5-F angiographic catheter to establish hepatic arterial anatomy, tumor location, and vascular supply. Feeding arteries supplying the target tumor were catheterized as selectively as possible using microcatheters. HAE was conducted using 40–300 μm microspheres (Embosphere; BioSphere Medical, Inc, Rockland, Massachusetts), but beginning with the smallest size particles. The endpoint of embolization was complete stasis of antegrade blood flow in the target vessels.

Imaging Technique

Procedures were performed in 3 different rooms using the same angiographic systems (Innova IGS 540, GE Healthcare) and an imaging workstation (Advantage Window, GE

Healthcare) loaded with the TFVDS (Flight Plan for Liver, GE Healthcare, Waukesha, WI, USA). Fluoroscopic and angiographic settings were similar across the rooms, and the same imaging protocol was used for all the procedures.

Multisegment DSA acquisitions were performed under breath hold and configured as follows: 4 frames per second (fps) for 5 s, then 2 fps for 5 s, and 1 fps for the rest of the time. Undiluted contrast media (Omnipaque 300, GE Healthcare) were injected during all DSA acquisitions with a flow rate ranging from 0.5 to 5 ml/s for 3–4 s depending on catheter position, vessel sizes, and flow.

For procedures where TFVDS was used, a CBCT was acquired with injection locations in the most proximal hepatic artery segment that would encompass the vessel's supplying tumor based on the patient's anatomy: common, proper, or left/right replaced or accessory hepatic artery. An initial DSA was always performed prior to the CBCT for optimizing injection parameters in an attempt to avoid reflux into the remainder of the more proximal arteries and to determine the optimal X-ray delay to visualize the tumors. Contrast injection rates for CBCT acquisitions varied from 1 to 4 ml/s depending on vessel size and flow, and the X-ray delay was from 4 to 6 s. The injection was maintained during the acquisition to ensure good filling of the arteries. For each single CBCT scan, the area of interest was centered and the arms of the patient were left by his or her side, following an institutional protocol. A rotation of 192° clockwise was performed under breath hold lasting for 5 s. Two-dimensional projections were automatically pushed to the workstation, and 0.48 mm by 22.4 cm axial slices were reconstructed in a 512 × 512 matrix size. Following a method previously described [10], the slices were loaded in TFVDS by a trained X-ray technologist, the suspected feeding vessel arteries highlighted using a 4-step workflow (Fig. 1), and results shown to the physician. For procedures where TFVDS was not used, 2D image guidance such as DSA overlay techniques was used. An immediate post-embolization CT or CBCT was performed at the end of each procedure to assess pattern of contrast retention in the tumor according to the institution standards [16].

Data and Imaging Analysis

The following baseline patient characteristics were obtained: gender, age, BMI, performance status, Child–Pugh class, BCLC stage, and tumor size and location. The following procedure characteristics were obtained: use of the TFVDS, procedure length (from access to closure), contrast volume and number of DSA, microspheres size, fluoroscopic time, and dose area product (DAP). The cumulated air kerma value for X-ray exposure measurement was not available for review. No reliable data

regarding the number of detected vessels in each case were available to allow comparison with those actually embolized.

Tumor response rates were measured according to modified Response Evaluation Criteria in Solid Tumors (mRECIST) criteria [17] on follow-up CT imaging by consensus of 2 radiologists (FC and AB) who were not involved in the procedures and blinded to the use of TFVDS. A contrast-enhanced CT was always obtained at 1 month to assess early tumor response, typically followed by CT scans every 3 months for the first year and then every 3 to 6 months, depending on disease stability. The radiologists also identified watershed tumors bridging two or more Couinaud–Bismuth segments of the liver on the initial CT scan performed before embolization [18].

Statistical Analysis

We compared results using the two-tailed Student's *t* test for continuous normally distributed data. The Fisher's exact and χ^2 tests were used for categorical data comparison (two-tailed). Tumor response was evaluated from the day of treatment until the date of last follow-up for each patient. Any enhancement observed within the target lesions during the follow-up was censored at the endpoint of the study. Complete response (CR) according to mRECIST corresponded to disappearance of any intratumoral arterial enhancement in target lesions, while partial response (PR) showed at least a 30% decrease in the sum of diameters of enhanced target lesions. Objective response (OR) included both CR and PR [19].

Differences in complete and objective response were tested in a univariate analysis with the following variables: guidance (TFVDS vs. DSA), tumor size (± 5 cm), tumor location (watershed vs. not watershed), number of tumors (single vs. multiple), and size of microspheres used (40–120 μm microspheres vs. 100–300 μm or both). Variables that showed statistical significance at univariate analysis were analyzed with a multivariate model where the risk (odds-ratio) of CR and objective response were estimated. A *p* value ≤ 0.05 was considered statistically significant. Data analysis was performed using STATA 12.0 (College Station, TX, USA).

Results

Patient Population

A total of 511 patients underwent HAE procedures during the 24-month study period. Among them, 93 had a first embolization performed for HCC, and 27 patients (19 males and 8 females, median age and range = 69 year,

Fig. 1 Tumor feeding vessels detection software workflow (FlightPlan for Liver, GE Healthcare) **A** Step 1—using the CBCT axial dataset, vessels are automatically segmented out from the bones. The cursor is positioned proximally on the tip of the catheter (*arrow*) in the hepatic arterial system to commence automatic vessel extraction. **B** Step 2—embolization target definition: A spherical region of interest is positioned over the hypervascular tumor region using 2D cross-sectional images (*arrowheads*: region of interest). **C** Step 3—isolation of relevant arterial vascular supply: Vessels are automatically detected and arteries supplying the designated hypervascular region of interest are highlighted in *color*. **D** Step 4—TFVDS export for live 3D roadmapping display: Extracted arterial vasculature is transferred to 3D roadmapping software to enable superimposition of the embolization plan on live fluoroscopy imaging

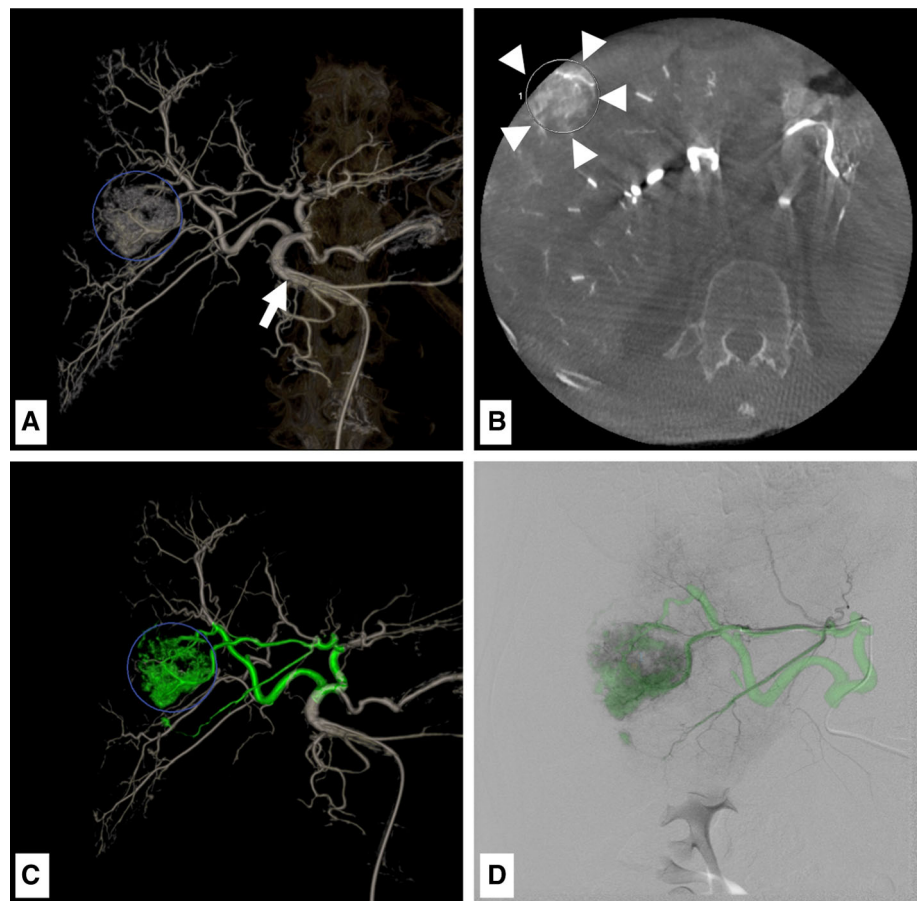


Table 1 Baseline patient and tumor characteristics

	Demographics
No. of patients/tumors	27/44
Gender (female/male)	8/19
Age (years)	69 (46–85)
HBs antigen (positive/negative)	6 (22%)/21 (78%)
HCV antibody (positive/negative)	14 (52%)/13 (48%)
Child–Pugh class (A/B)	26 (96%)/1 (4%)
BCLC	A: 15, B: 10, C: 2
Size (mm)	38 (6–100)
Number of tumors (1/2/3/4)	2 (1–4)
Location	I: 1, II: 2, III: 4, IV: 9, V: 3, VI: 5, VII: 5, VIII: 11, VI/VII: 1, VIII/IV: 3
Body mass index	24.6 (17–50.1)
Variant anatomy	I (21)/II (2)/III (2)/V

Data are expressed as the median (range)

Variant anatomy according to Michel et al. (Favelier S, Germain T, Genson PY, et al. (2015) Anatomy of liver arteries for interventional radiology. Diagnostic and interventional imaging, 96(6):537–546)

HB hepatitis B; HCV hepatitis C virus

46–85) with 44 tumors fulfilled the inclusion and exclusion criteria for this study. Baseline patient and tumor characteristics are presented in Table 1.

Procedure Analysis

There were 13 and 14 patients (19 and 25 tumors) treated using TFVDS guidance or DSA alone, respectively. Procedure characteristics, reported in Table 2, did not differ significantly, except for DAP with 149.7 Gy.cm² (38–365) in cases using TFVDS versus 227.8 gy.cm² (85.3–468.6) when using 2D imaging only ($p = 0.05$). A total of 31 tumors was embolized by 40–120 μ m microspheres; 9 with 100–300 μ m microspheres; and 4 using both ranges of size of microspheres. No adverse event was reported.

Tumor Response

The median follow-up time was 20.1 months (range = 2–33 months) for all patients. Univariate and multivariate analyses are reported in Table 3. No factors were predictive of the objective response as observed in 88.6% (39–44) of the treated tumors. A higher rate of CR was observed for HAE using TFVDS versus DSA (68.4%, 13–19, vs. 36%, 9–25, $p = 0.03$) (Figs. 2, 3). HAE using TFVDS was the only predictive factor of CR on univariate analysis (odds-ratio; 3.85 [confidence interval, CI: 95%: 1.09, 13.67], $p = 0.04$) but not on multivariate analysis (odds-ratio = 3.26 [0.87, 12.23], $p = 0.08$).

Discussion

In this study, our results demonstrated that TFVDS may be associated with improved tumor response in patients with HCC who are treated selectively with bland embolization. Using DSA alone, physicians usually identify tumor feeding vessels sequentially, which may be challenging due to the potential development during the procedure of spasm or reflux of embolic material in remaining vessels supplying the tumor [20]. Identifying all vessels feeding the tumors using CBCT with or without TFVDS prior to guidewire manipulation or injection of embolic agent in any one vessel prevents this problem [6, 10]. Manually identifying tumor feeding vessels using DSA alone or CBCT can be time-consuming [11] and subjective. DSA images are a planar projection of both vessels and tumor blush, and the analysis remains limited by the potential misidentification or poor visualization of tumor vessels, mainly due to superimposed vessels [9]. CBCT by itself offers consistent 3D visualization of the liver vessels with high vessel-to-liver contrast and high spatial resolution. Its sensitivity for the detection of feeders has been found to range between 73 and 100% compared to 50–72% with DSA, resulting in a modification of treatment delivery in 28–81% of the procedures [9]. TFVDS can detect tumor feeding vessels with even greater sensitivity. It can semiautomatically identify 29–50% and 7–20% more feeders than can be detected by DSA and CBCT alone, respectively [6, 9–11, 21, 22]. Previous studies have shown that the high

Table 2 Baseline procedure characteristics

	TFVDS TAE	DSA TAE	<i>p</i> value
Number of DSA	10.3 (5–15)	11.9 (8–16)	0.30
Procedural time (min)	136 (64–270)	106 (72–174)	0.09
Fluoroscopy time (min)	37 (19–100)	31.5(19–56)	0.81
Dose area product (Gy.cm ²)	149.75 (38–365)	227.8 (85.3–468.62)	0.05
Contrast volume	170.08 (80–360)	152.69 (100–225)	0.68

Note—data are expressed as the mean (range); TFVDS: tumor feeding vessel detection software; DSA: digital subtraction angiography; HAE: hepatic arterial embolization

Table 3 Univariate and multivariate analyses

Variable	Univariate Analysis			Multivariate Analysis		
	OR	CI95%	<i>p</i> value	OR	CI95%	<i>p</i> value
Guidance (TFVDS vs. DSA)	3.85	1.09;13.67	0.04	3.37	0.79;14.41	0.1
Number of tumors (single vs. multiple)	1	0.28; 3.56	1	–	–	–
Size (size \pm 5 cm)	2.96	0.65;13.4	0.16	–	–	–
Location (watershed vs. not)	1	0.18;5.6	1	–	–	–
Microspheres size (40–120 μ m vs. 100–300 μ m or both)	1.244	0.34;4.56	0.74	–	–	–

Note—only examined variables displaying significance at univariate analysis were evaluated at multivariate analysis. Multivariate analysis data were calculated with the regression model. TFVDS: tumor feeding vessel detection software; DSA: digital subtraction angiography; OR: odds-ratio; CI95%: confidence intervals 95%

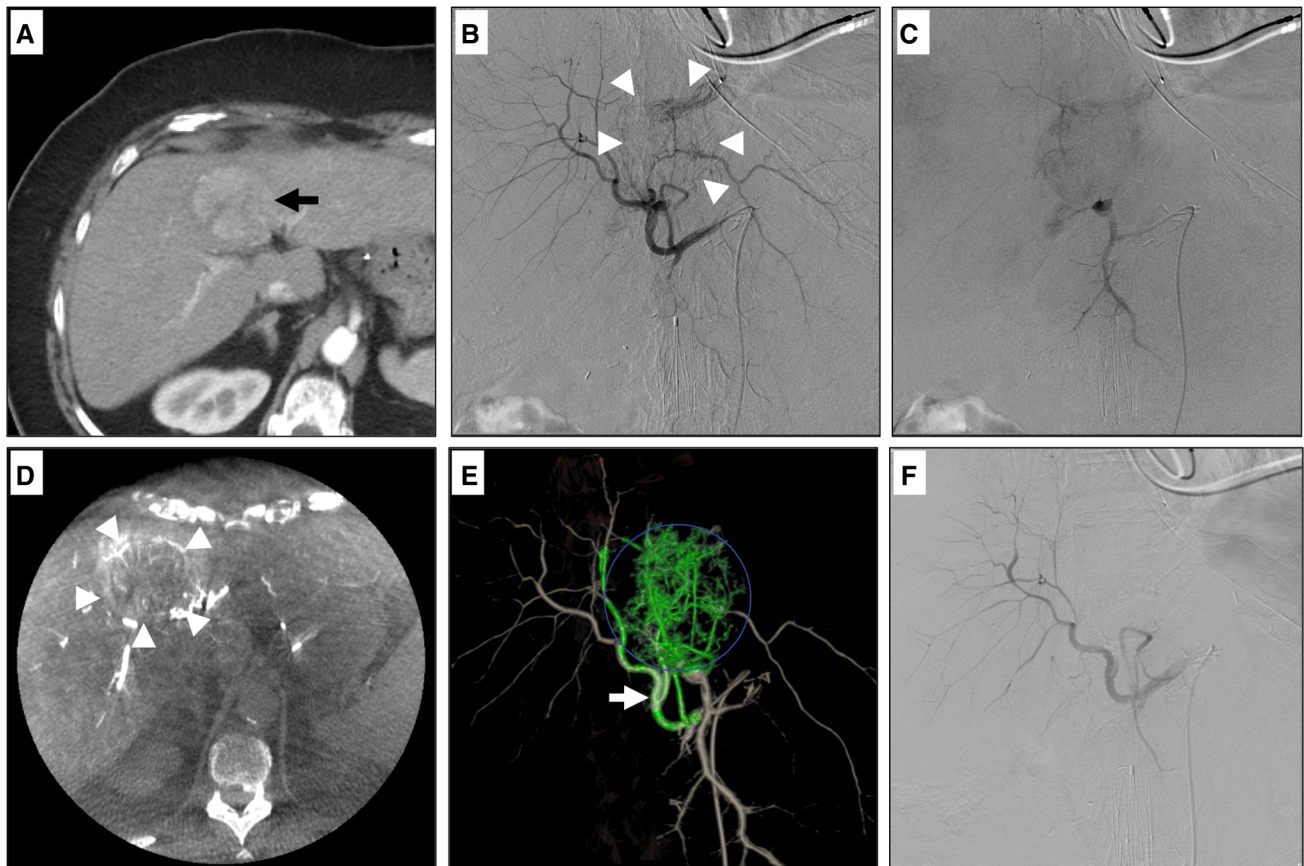


Fig. 2 Successful bland transarterial embolization using tumor feeding vessel detection software. Hepatocellular carcinoma in a 77-year-old woman located in segment IV. **A** Preoperative contrast-enhanced CT scan shows the highly vascularized tumor (*black arrow*). **B** DSA shows ill-defined tumor vascular blushes (*arrowheads*). **C** Corresponding DSA shows tumor vascular blushes on late phase. **D** Contrast-enhanced CBCT clearly depicts the tumors as a focal hypervascular nodule (*arrowheads*) and allows visualization of

the tumor feeder vessels. **E** After segmentation of the hepatic arteries, the software highlighted in green the vessels running between the tip of the catheter placed in the hepatic artery and the target. This allowed 3D visualization of the tumor feeding vessels (*white arrow*). **F** Final DSA did not show residual tumor feeding vessels. The subsequent follow-up CT scan identified no residual enhancement leading to a complete response according to mRECIST classification

sensitivity of TFVDS can be counterbalanced by a low specificity or vice versa, if the size and position of the ROI surrounding a tumor are not optimally chosen [11]. Following the recommendation from Iwazawa et al., the ROI surrounding a tumor (Fig. 3) was always sized to fit the tumor. Nevertheless, none of the previous studies have compared the post-embolization clinical outcomes of using dedicated software vs. other imaging techniques. By using a vessel tracking software with CBCT to provide a 3D semiautomatic assessment, unnecessary treatment due to poor vessel selection or insufficient treatment due to failure to identify tumor feeders can be limited. In our study, a significant higher rate of CR was observed for HAE using TFVDS versus DSA, and HAE using TFVDS was the only predictive factor of CR on univariate analysis. The absence of statistical differences on OR might be related to the fact that bland embolization used to be effective even partially.

The lack of statistical significance of CR on multivariate analysis may be related to the lack of statistical power.

Iwazawa et al. [11] reported that TFVDS software-assisted transarterial chemoembolization for HCC reduced the number of DSA acquisitions, and for single tumors only treatment could be completed in a shorter time, while maintaining a comparable treatment response in comparison with software-unassisted transarterial chemoembolization. In our study, we did not find any significant differences in the number of DSA acquisitions performed or procedure time between the TFVDS and the DSA only groups, which could be due to different patient baseline characteristics, in particular the number of tumors per patient and size of tumors. On the other hand, we demonstrated a reduced DAP for the TFVDS group, likely due to the combination of reduced, but not significant, BMI and number of acquisitions in this group.

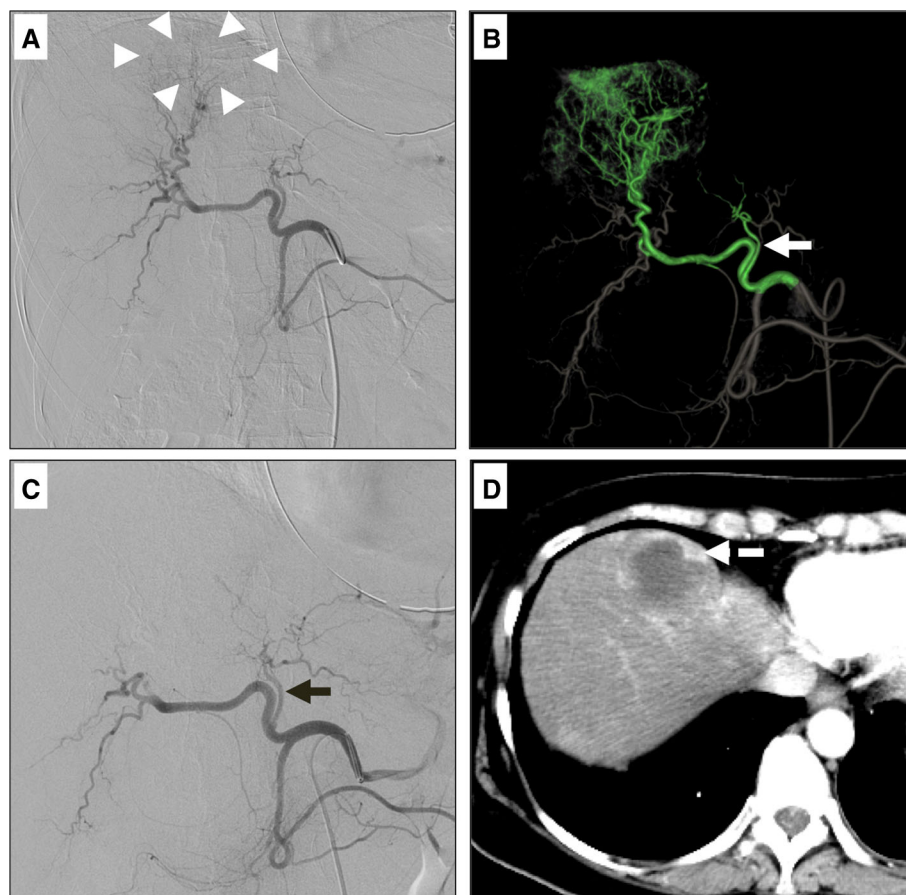


Fig. 3 Partial response after transarterial embolization using tumor feeding vessel detection software. Hepatocellular carcinoma in a 62-year-old woman with hepatitis B-related cirrhosis located in segment IVA. **A** DSA shows ill-defined tumor vascular blushes (*arrowheads*). **B** After segmentation of the hepatic arteries visualized on contrast-enhanced cone beam CT, the software highlighted in green the vessels running between the tip of the catheter placed in the hepatic artery and the target tumor. This allowed 3D visualization of

one main and one secondary tumor feeding vessels (*white arrow*). However, only the main vessel was embolized based on the physician's decision. **C** Final DSA showed the non-embolized residual tumor feeding vessel (*black arrow*). **D** Subsequent contrast-enhanced CT scan identified residual viable tissue within the tumor (*dashed arrow*) leading to partial response according to mRECIST classification

This study is limited by its retrospective nature and the small number of patients studied. While there is no gold standard for the identification of tumor feeding vessels in the interventional room, DSA was used as the reference even though 3D imaging has been shown to be superior to 2D imaging for the identification of tumor feeding vessels [6]. Lastly, the utility of TFDVS could not be separated from utility of CBCT alone in our retrospective study since the TFDVS was always used when a CBCT was performed. Further studies might compare the impact of such software with CBCT manual analysis in addition to 2D imaging.

In conclusion, HAE using TFDVS may result in better local tumor response than DSA alone for patients with HCC. A prospective validation on a larger scale is now needed before drawing definitive conclusions.

Acknowledgements The authors thank Gregoire Avignon, Clinical Research Engineer at GE Healthcare, for his technical support.

Funding This study was funded in part through the NIH/NCI Cancer Center Support Grant P30 CA008748.

Compliance with Ethical Standards

Conflict of interest The authors declare that they have no conflict of interest.

Ethical Approval All procedures performed in studies involving human participants were in accordance with the ethical standards of the institutional and/or national research committee and with the 1964 Helsinki Declaration and its later amendments or comparable ethical standards.

Informed Consent Informed consent was waived for all individual participants included in the study.

References

- Mauri G, Varano GM, Orsi F. TAE for HCC: when the old way is better than the new ones!!! *Cardiovasc Intervent Radiol.* 2016;39(6):799–800.
- Bonomo G, Pedicini V, Monfardini L, et al. Bland embolization in patients with unresectable hepatocellular carcinoma using precise, tightly size-calibrated, anti-inflammatory microparticles: first clinical experience and one-year follow-up. *Cardiovasc Intervent Radiol.* 2010;33(3):552–9.
- Bonomo G, Della Vigna P, Monfardini L, et al. Combined therapies for the treatment of technically unresectable liver malignancies: bland embolization and radiofrequency thermal ablation within the same session. *Cardiovasc Intervent Radiol.* 2012;35(6):1372–9.
- Racadio JM, Babic D, Homan R, et al. Live 3D guidance in the interventional radiology suite. *AJR Am J Roentgenol.* 2007;189(6):W357–64.
- Iwazawa J, Ohue S, Hashimoto N, Muramoto O, Mitani T. Survival after C-arm CT-assisted chemoembolization of unresectable hepatocellular carcinoma. *Eur J Radiol.* 2012;81(12):3985–92.
- Ronot M, Abdel-Rehim M, Hakime A, et al. Cone-beam CT angiography for determination of tumor-feeding vessels during chemoembolization of liver tumors: comparison of conventional and dedicated-software analysis. *J Vasc Interv Radiol.* 2016;27(1):32–8.
- Tacher V, Radaelli A, Lin M, Geschwind JF. How I do it: cone-beam CT during transarterial chemoembolization for liver cancer. *Radiology.* 2015;274(2):320–34.
- Pellerin O, Lin M, Bhagat N, Shao W, Geschwind JF. Can C-arm cone-beam CT detect a micro-embolic effect after TheraSphere radioembolization of neuroendocrine and carcinoid liver metastasis? *Cancer Biother Radiopharm.* 2013;28(6):459–65.
- Bapst B, Lagadec M, Breguet R, Vilgrain V, Ronot M. Cone beam computed tomography (CBCT) in the field of interventional oncology of the liver. *Cardiovasc Intervent Radiol.* 2016;39(1):8–20.
- Deschamps F, Solomon SB, Thornton RH, et al. Computed analysis of three-dimensional cone-beam computed tomography angiography for determination of tumor-feeding vessels during chemoembolization of liver tumor: a pilot study. *Cardiovasc Intervent Radiol.* 2010;33(6):1235–42.
- Iwazawa J, Ohue S, Hashimoto N, Mitani T. Comparison of the number of image acquisitions and procedural time required for transarterial chemoembolization of hepatocellular carcinoma with and without tumor-feeder detection software. *Radiol Res Pract.* 2013;2013:580839.
- European Association for the Study of the Liver. EASL-EORTC clinical practice guidelines: management of hepatocellular carcinoma. *Eur J Cancer (Oxford, England: 1990).* 2012;48(5):599–641.
- Brown KT, Do RK, Gonen M, et al. Randomized trial of hepatic artery embolization for hepatocellular carcinoma using doxorubicin-eluting microspheres compared with embolization with microspheres alone. *J Clin Oncol Off J Am Soc Clin Oncol.* 2016;34(17):2046–53.
- Facciorusso A, Bellanti F, Villani R, et al. Transarterial chemoembolization vs bland embolization in hepatocellular carcinoma: a meta-analysis of randomized trials. *United Eur Gastroenterol J.* 2017;5(4):511–8.
- Massarweh NN, Davila JA, El-Serag HB, et al. Transarterial bland versus chemoembolization for hepatocellular carcinoma: rethinking a gold standard. *J Surg Res.* 2016;200(2):552–9.
- Wang X, Erinjeri JP, Jia X, et al. Pattern of retained contrast on immediate postprocedure computed tomography (CT) after particle embolization of liver tumors predicts subsequent treatment response. *Cardiovasc Intervent Radiol.* 2013;36(4):1030–8.
- Jung E, Kim J, Yoon E, et al. The optimal tumor response assessment in patients with HCC after treatment of TACE. *J Clin Oncol Off J Am Soc Clin Oncol.* 2011;29(4_suppl):215.
- Kothary N, Takehana C, Mueller K, et al. watershed hepatocellular carcinomas: the risk of incomplete response following transhepatic arterial chemoembolization. *J Vasc Interv Radiol.* 2015;26(8):1122–9.
- Vincenzi B, Di Maio M, Silletta M, et al. Prognostic relevance of objective response according to EASL criteria and mRECIST criteria in hepatocellular carcinoma patients treated with loco-regional therapies: a literature-based meta-analysis. *PLoS ONE.* 2015;10(7):e0133488.
- Basile A, Carrafiello G, Ierardi A, Tsetis D, Brountzos E. Quality-improvement guidelines for hepatic transarterial chemoembolization. *Cardiovasc Intervent Radiol.* 2012;35:765–74.
- Miyayama S, Yamashiro M, Hashimoto M, et al. Identification of small hepatocellular carcinoma and tumor-feeding branches with cone-beam CT guidance technology during transcatheter arterial chemoembolization. *J Vasc Interv Radiol.* 2013;24(4):501–8.
- Minami Y, Yagy Y, Murakami T, Kudo M. Tracking navigation imaging of transcatheter arterial chemoembolization for hepatocellular carcinoma using three-dimensional cone-beam CT angiography. *Liver Cancer.* 2014;3(1):53–61.